RESEARCH PAPER

Cholesteryl butyrate solid lipid nanoparticles inhibit the adhesion and migration of colon cancer cells

R Minelli[1], L Serpe[1], P Pettazzoni[2], V Minero[2], G Barrera[2], CL Gigliotti[3], R Mesturini[3], AC Rosa[1], P Gasco[4], N Vivenza[4], E Muntoni[1], R Fantozzi[1], U Dianzani[3], GP Zara[1] and C Dianzani[1]

[1]*Dipartimento di Scienza e Tecnologia del Farmaco, Università di Torino, Torino, Italy,* [2]*Dipartimento di Medicina e Oncologia Sperimentale, Sezione di Patologia Generale, Università di Torino, Torino, Italy,* [3] *Dipartimento di Scienze Mediche, Università del Piemonte Orientale, 'A. Avogadro', Novara, Italy, and* [4]*Nanovector s.r.l., Torino, Italy*

BACKGROUND AND PURPOSE

Cholesteryl butyrate solid lipid nanoparticles (cholbut SLN) provide a delivery system for the anti-cancer drug butyrate. These SLN inhibit the adhesion of polymorphonuclear cells to the endothelium and may act as anti-inflammatory agents. As cancer cell adhesion to endothelium is crucial for metastasis dissemination, here we have evaluated the effect of cholbut SLN on adhesion and migration of cancer cells.

EXPERIMENTAL APPROACH

Cholbut SLN was incubated with a number of cancer cell lines or human umbilical vein endothelial cells (HUVEC) and adhesion was quantified by a computerized micro-imaging system. Migration was detected by the scratch 'wound-healing' assay and the Boyden chamber invasion assay. Expression of ERK and p38 MAPK was analysed by Western blot. Expression of the mRNA for E-cadherin and claudin-1 was measured by RT-PCR.

KEY RESULTS

Cholbut SLN inhibited HUVEC adhesiveness to cancer cell lines derived from human colon–rectum, breast, prostate cancers and melanoma. The effect was concentration and time-dependent and exerted on both cancer cells and HUVEC. Moreover, these SLN inhibited migration of cancer cells and substantially down-modulated ERK and p38 phosphorylation. The anti-adhesive effect was additive to that induced by the triggering of B7h, which is another stimulus inhibiting both ERK and p38 phosphorylation, and cell adhesiveness. Furthermore, cholbut SLN induced E-cadherin and inhibited claudin-1 expression in HUVEC.

CONCLUSION AND IMPLICATIONS

These results suggest that cholbut SLN could act as an anti-metastastic agent and they add a new mechanism to the anti-tumour activity of this multifaceted preparation of butyrate.

Abbreviations

Cholbut, cholesteryl butyrate; Cholpalm, cholesteryl palmitate; CRC, colorectal carcinoma; EC, vascular endothelial cell; FCS, fetal calf serum; GAPDH, glyceraldehyde-3-phospate dehydrogenase; HDAC, histone deacetylase; MCT1, monocarboxylate transporter 1; PMA, phorbol 12-myristate 13-acetate; PMNs, polymorphonuclear cells; SCFAs, short-chain fatty acids; SLN, solid lipid nanoparticles; SMCT1, sodium-coupled monocarboxylate transporter 1

Introduction

Colorectal carcinoma (CRC) is one of the most frequent malignancies in both men and women in the Western world, in terms of both incidence and mortality (O'Neil and Goldberg, 2008). The propensity of CRC cells to invade surrounding tissues and metastasize to other organs is responsible for most deaths. The majority of CRCs are sporadic, and dietary risk factors are involved in their development. Epidemiological evidence suggests that a high-fibre diet is protective (Giovannucci *et al.*, 1992; Scharlau *et al.*, 2009), whose fermentation by colonic flora yields short-chain fatty acids (SCFAs) postulated to be important protective factors. The concentration of SCFAs may reach approximately 100 mM in the colon lumen and butyrate constitutes about 20–30% of these SCFAs (Cummings, 1981). Butyrate is taken up by colon epithelial cells and serves as a major source of energy for the colon mucosa. It stimulates fluid and electrolyte absorption, inhibits colon inflammation and oxidative stress, improves the colon's defence barriers and inhibits colon carcinogenesis (Gonçalves *et al.*, 2009). The absence of butyrate is associated with mucosal atrophy and death of the colon cells. Butyrate has received close attention as a potential chemopreventive agent (Wollowski *et al.*, 2001; Delzenne *et al.*, 2003), especially because *in vitro* exposure of tumour cells to this agent has been shown to induce apoptosis, inhibit proliferation and promote differentiation (Kobayashi *et al.*, 2003), not only in CRC cells but also in breast, gastric, lung, brain and pancreas cancer cells (Brioschi *et al.*, 2008). Sodium butyrate is an inhibitor of histone deacetylase (HDAC) and has displayed some efficacy as an anti-tumour drug in phase I and phase II clinical trials (Minucci and Pelicci, 2006). Unfortunately, its clinical use is limited by its short half-life, which is due to its rapid metabolism through the liver and rapid excretion (Pellizzaro *et al.*, 1999). This requires its continuous parenteral administration to maintain therapeutic concentrations. Furthermore, adverse events (such as anaemia, headache, nausea, diarrhoea, abdominal cramps and strong odour) further reduce patient compliance.

The formation of clinically detectable tumour metastasis involves several steps that proceed in a defined sequence. Survival of the primary tumour beyond a certain size requires the production of angiogenic factors inducing the vascularization of the tumour mass. The next step is dissemination of tumour cells in the bloodstream and their homing to the site of the metastasis, where the tumour cell must proliferate in order to produce a detectable metastasis. Although the rate-limiting step of this process is unknown, the adhesion of the tumour cells to the vascular endothelium and the subsequent extravasation at the site of metastasis seem to be of crucial importance (Weiss, 1990). This process involves molecular interactions similar to those used in the course of leucocyte recruitment into tissues, which is crucial for the inflammatory and immune responses. This process is regulated by adhesion receptors and their ligands, whose expression and function are finely regulated in both vascular endothelial cells (EC) and leucocytes according to cell type, functional state and anatomical location, and it builds up a complex network of interactions that simultaneously involve several adhesion receptors (Dianzani and Malavasi, 1995; Laferrière *et al.*, 2001; 2004; Ley *et al.*, 2007). The function of these adhesion receptors is mainly regulated by modulating their expression level, but some of them also modulate their intrinsic adhesiveness in response to activating stimuli. They cooperate in a multistep process involving (i) cell rolling on the EC surface, mediated by selectins; (ii) activation of integrins from a low to a high adhesive conformation, mediated by chemokines; (iii) cell arrest, mediated by integrins; and (iv) extravasation, mediated by integrins and other molecules such as CD31, JAM-A and CD44. However, this schematic picture underestimates the complexity of the process, as several adhesion molecules play roles in many steps.

Solid lipid nanoparticles (SLN) have been extensively studied as promising innovative carriers for drugs and diagnostics (Westesen *et al.*, 1997; Gasco, 2001; Dianzani *et al.*, 2006). In the field of oncology, their use has been already evaluated in preclinical and clinical trials, and even approved for clinical use in some instances (Manjunath *et al.*, 2005). SLN, prepared from a warm microemulsion and carrying a drug (either hydrophilic or lipophilic), have been tested *in vivo* in animals via duodenal, i.v. and ocular administration (Dianzani *et al.*, 2006; Brioschi *et al.*, 2008). SLN can increase bioavailability and modify the pharmacokinetics and tissue distribution of the incorporated drug. Generally, the lipophilic matrix consists of fatty acids and/or triglycerides (Gasco, 2001). Cholesteryl butyrate (cholbut) SLN have been prepared using the microemulsion method (Matsumura and Kataoka, 2009); they have a spherical shape with an average diameter of around 80 nm, and they have been extensively studied as a pro-drug of butyric acid (Gasco, 2004). In several tumour cell lines, they were internalized within a few minutes and displayed a greater anti-neoplastic effect than that of butyrate (Westesen *et al.*, 1997; Salomone *et al.*, 2001; Serpe *et al.*, 2004).

In earlier work (Dianzani *et al.*, 2006), we showed that cholbut SLN inhibited the adhesion of polymorphonuclear cells (PMNs) to HUVEC, and we suggested that they may be used as anti-inflammatory agents in chronic inflammatory diseases. The aim of the research reported here was to extend the analysis and assess the anti-metastatic potential of cholbut SLN, as tumour cell adhesion to EC – which is crucial for their metastatic dissemination – uses mechanisms similar to those used by PMNs (Dianzani *et al.*, 2010). The results showed that cholbut SLN strikingly decreased adhesion of tumour cell lines to human umbilical vein endothelial cells (HUVEC) and the migration of cancer cells. These effects seemed to be mediated by inhibition of the ERK and p38 pathways on HUVEC and tumour cell lines, and they supported the possible efficacy of cholbut SLN in anti-cancer therapy.

Methods

Preparation of cholbut SLN and sodium butyrate solutions

Cholbut SLN were prepared by the microemulsion method reported elsewhere (Pellizzaro *et al.*, 1999) and described in PATENT WO0030620. Briefly, a warm oil-in-water microemulsion was prepared from cholesteryl butyrate (Asia Talent Chemical, Shenzen, China), Epikuron 200 (Cargill, Milan, Italy), sodium glycocholate and water; 2-phenylethanol was added as a preservative. The warm microemulsion was dis-

persed in cold water, and the resulting cholbut SLN aqueous dispersion was washed three times by dia-ultrafiltration using a Vivaflow50 membrane (Sartorius Stedim Biotech GmbH, RC; cut-off 100 000 Da) (Serpe et al., 2010). The aqueous dispersions of cholbut SLN were sterilized by 0.2 μm filtration before use.

Solutions of sodium butyrate were freshly prepared in sterile water before each experiment, at a concentration of 5 M.

Fluorescence microscopy

Fluorescent cholbut SLN was prepared by adding 6-coumarin (Acros, Morris Plain, NJ) (0.04%). The microemulsion was subsequently dispersed in cold water, washed by ultrafiltration and sterilized. The cellular uptake of 6-coumarin-tagged cholbut SLN by HT29 cells was then investigated using fluorescence microscopy. Briefly, 25×10^3 HT29 cells were seeded in 1 mL of culture medium in 24-well plates and were allowed to attach for 24 h on glass coverslips in the wells. 4′,6′-diamidino-2-phenylindole (DAPI; 1 μg·mL^{-1}) (Sigma-Aldrich, Milan, Italy) was used as nuclear staining. After 15 min incubation with 100 μM fluorescent cholbut SLN, the cells were washed with PBS solution, and the coverslips were inverted and mounted on glass slides. Cells were observed and photographed by Leica fluorescence microscope DM IL (Leica Microsystems, Wetzlar, Germany).

Cell culture

HUVEC were isolated from human umbilical veins (informed consent was obtained from all donors) by trypsin treatment (1%) and cultured in M199 medium with the addition of 20% fetal calf serum (FCS) and 100 U·mL^{-1} penicillin, 100 μg·mL^{-1} streptomycin, 5 UI·mL^{-1} heparin, 12 μg·mL^{-1} bovine brain extract and 200 mM glutamine. HUVEC were grown to confluence in flasks and used between the second and fifth passages. EC viability was not affected by the drug treatment.

HT29, HCT116 and CaCo-2 cells derived from human colon adenocarcinoma and MCF-7 cells from human breast carcinoma were obtained from American Type Culture Collection (Manassas, VA). PC-3 cells from human prostate carcinoma was a gift by Dr Pili (Roswell Park Cancer Institute, Buffalo, NY), and M14 and LM cells, from human melanoma were a gift by Dr Pistoia (Gaslini Institute, Genoa). The human tumour cell lines were grown in culture dishes as a monolayer in RPMI 1640 medium plus 10% FCS, 100 U·mL^{-1} penicillin and 100 μg·mL^{-1} streptomycin at 37°C in a 5% CO$_2$ humidified atmosphere.

Cell surface phenotype was assessed by immunofluorescence and flow cytometry using the appropriate FITC- and PE-conjugated mAb to ICAM-1 (Biolegend, San Diego, CA, USA), ICAM-2 (Diaclone Research, San Diego, CA, USA), MadCAM (Abcam, Cambridge, UK), CD62P (Immunotools, Friesoythe, Germany) and Sialyl Lewis X (Santa Cruz Biotechnology, Santa Cruz, CA, USA). MAb to CD62E (ImmunoKontact, Abingdon, UK), Sialyl Lewis A (Santa Cruz Biotechnology) and VCAM-1 (Caltag-Medsystem, Buckingham, UK) were detected with FITC-conjugated goat anti-mouse-Ig (Caltag).

Cell adhesion assay

HUVEC were grown to confluence in 24-well plates, washed and rested for 1 day in M199 plus 10% FCS. In most experi-

ments, they were incubated or otherwise with increasing concentrations of cholbut SLN, sodium butyrate and cholpalm SLN (0.1–100 μM) for 10 min–48 h, washed with fresh medium twice and incubated for 1 h with the tumour cells (1×10^5 cells per well); the 1 h incubation time was chosen to allow full sedimentation of the adhering cells, but similar results were obtained with shorter incubation times (10 and 20 min). After incubation, non-adherent cells were removed by being washed three times with M199. The centre of each well was analysed by fluorescence image analysis (Dianzani et al., 2006). Adherent cells were counted by the Image Pro Plus Software for micro-imaging (Media Cybernetics, version 5.0, Bethesda, MD, USA). Single experimental points were assayed in triplicate, and the standard error of the three replicates was always below 10%. Data are shown as percentages of the inhibition of treated cells versus the control adhesion measured on untreated cells; this control adhesion was 40 ± 4 cells per microscope field ($n = 17$) for HT29 cells and in a similar range for the other cell types.

In some experiments, HUVEC were treated with SB203580 (10 μM) or PD98059 (10 μM) (p38 and ERK inhibitors, respectively) in the presence and absence of cholbut SLN (10 μM) for 24 h. Cells were then washed and incubated with HT29 for 1 h. In a few experiments, HUVEC were pre-activated with IL-1β (0.01 μM) for 1 h and then exposed or not exposed to cholbut SLN for a further 24 h.

In other experiments, only the cancer cells were treated with cholbut SLN. HT29 or HCT116 cells were treated with increasing concentrations of cholbut SLN (0.1–100 μM) for 8–48 h, washed with fresh medium twice and then incubated for 1 h with untreated HUVEC. We also assessed the effect of treating both HT29 cells and HUVEC with cholbut SLN. In these experiments, cells were separately treated with increasing concentrations of cholbut SLN (0.1–10 μM) for 24 h, washed with fresh medium twice and incubated together for 1 h.

In the experiments assessing the combined effect of cholbut SLN and ICOS-Fc, HUVEC were treated with ICOS-Fc (0.5–0.1 μg·mL^{-1}) and/or cholbut SLN (0.3–1 μM) for 24 h, washed with fresh medium twice and incubated for 1 h with HT29 cells. ICOS-Fc is a recombinant protein composed of the extracellular portion of the T-cell co-stimulatory receptor ICOS (inducible co-stimulator) and the Fc portion of human IgG1.

Cell motility assay

To assess the effect of cholbut SLN and sodium butyrate on PC-3 cell motility, we carried out standard wound-healing experiments. In brief, cells were plated onto six-well plates (at a concentration of 10^6 cells per well) and grown to confluence. PC-3 cells were then left for 12 h with FCS free-medium (to prevent cell proliferation). Cell monolayers were carefully wounded by scratching with a sterile plastic pipette tip along the diameter of the well (as illustrated in the Results). The cells were washed twice with FCS-free medium before their subsequent incubation with culture medium in the absence (control) or presence of cholbut SLN or sodium butyrate at appropriate concentrations. In order to monitor cell movement into the wounded area, five fields of each of the three wounds analysed per condition were photographed

immediately after the scratch was made (0 h) and 24 and 48 h later.

Matrigel invasion area

In order to determine the effects of cholbut SLN on cell invasiveness, we used the Boyden chamber (BD Biosciences, Milan, Italy) invasion assay. PC-3, HT29 and HCT116 cells (8000) were plated onto the apical side of Matrigel-coated (50 µg·mL^{-1}) filters in serum-free medium with or without cholbut SLN or sodium butyrate (1–100 µM). Medium containing 20% FCS was placed in the basolateral chamber as a chemoattractant. After 8 h, the cells on the apical side were wiped off with Q-tips. Cells on the bottom of the filter were stained with crystal violet and counted (five fields of each triplicate filter) with an inverted microscope. Results are expressed as the number of migrated cells per high-power field.

In some experiments, HT29 cells were treated with SB203580 or PD98059 (10 µM) with or without cholbut SLN 10 µM for 8 h and then used in the invasion assay.

Protein extraction and Western blot analysis

In order to stimulate ERK and p38 activation, cholbut SLN-treated and untreated HUVEC were exposed to 0.01 µM VEGF-A for 10 min, whereas cholbut SLN-treated and untreated HT29 cells were exposed to 0.01 µM phorbol 12-myristate 13-acetate (PMA) for 10 min.

In order to evaluate the effect of cholbut SLN on acetyl-H3 and p21^{CIP1} expression level, HT29 cells were treated with 5 mM sodium butyrate, or 0.1 µM Trichostatin A, or 100 µM cholbut SLN, and the expression levels of acetyl-H3 and p21^{CIP1} were analysed by Western blot in the cell lysates.

Cells were lysed in a buffer composed of 50 mM Tris–HCl, pH 7.4, 150 mM NaCl, 5 mM EDTA, 1% NP40, phosphatase and protease inhibitor cocktails. Cell lysates were then cleared from insoluble fractions through high-speed centrifugation, and protein concentrations were determined with a commercially available kit (Bio-Rad Laboratories, Milan, Italy). 10–40 µg proteins were loaded on 10% SDS-PAGE gels and, after electrophoresis, transferred onto nitrocellulose membranes. These were blocked by incubation for 1 h at room temperature with 5% non-fat milk dissolved in TBS Tween 20. The membranes were then probed overnight with primary antibodies and, after three washes, incubated for 1 h with HRP-conjugated secondary antibodies. Bands were detected by chemiluminescence, and densitometric analysis was performed with the Multi-Analyst software (version 1.1, Bio-Rad Laboratories).

RNA isolation and SYBR Green real time RT-PCR

In order to clarify the cholbut SLN effect on cadherin and claudin-1, the expression level of the mRNA was measured after 4, 8 and 24 h of incubation with 100 µM cholbut SLN by quantitative SYBR Green real-time RT-PCR. Total RNA was obtained from HT29 and HUVEC using the RNeasy Plus Mini Kit (Qiagen, Milan, Italy) according to the manufacturer's instructions. The RNA concentrations were quantified with the Qubit Fluorometer (Invitrogen, Milan, Italy). The Quant-iT RNA Assay Kit (Invitrogen) was used, and calibration was performed using a two-point standard curve according to

the manufacturer's instructions. QuantiTect Primer Assay (Qiagen) was used as the gene-specific primer pair for human E-cadherin *CDH1* (cat. no. QT00080143), claudin-1 *CLDN1* (cat. no. QT00225764). Real-time RT-PCR analysis was carried out using 100 ng of total RNA, which was reverse transcribed in a 20 µL cDNA reaction using the QuantiTect Reverse Transcription Kit (Qiagen) according to the manufacturer's instructions; 10 ng of cDNA was used for each 25 µL real-time RT-PCR reaction. Quantitative RT-PCR was performed using the QuantiTect SYBR Green RT-PCR Kit (Qiagen). To normalize mRNA data, the transcript of the housekeeping gene glyceraldehyde-3-phosphate dehydrogenase (GAPDH) (cat. no. QT01192646) was used, and real-time PCR was performed by a MiniOpticon Real Time PCR system (Bio-Rad, Milan, Italy). The PCR protocol conditions were as follows: HotStarTaq DNA polymerase activation step at 95°C for 15 min, followed by 40 cycles at various temperatures/times (i.e. 94°C for 15 s, 55°C for 30 s and 72°C for 30 s). All samples were run in duplicate. At least two non-template controls were included in all PCR runs. The quantification data analyses were performed using the Bio-Rad CFX Manager Software version 1.6 (Bio-Rad) in accordance with the manufacturer's instructions. These analyses were performed following the MIQE guidelines (Minimum Information for Publication of Quantitative Real-time PCR Experiments) (Bustin *et al.*, 2009).

Data analysis

Data are shown as mean ± SEM or mean ± SD for mRNA expression. Statistical analyses were performed with Graph-Pad Prism 3.0 software (La Jolla, CA, USA) using one-way ANOVA and Dunnett's test. Values of $P < 0.05$ were considered statistically significant.

Materials

Cholbut and cholesteryl palmitate SLN were produced by Dr Gasco (Nanovector s.r.l. Turin, Italy). FCS (endotoxin tested) was from Hyclone Laboratories (Milan, Italy). Trypsin was from Difco Laboratories (Milan, Italy). M199, RPMI, IL-1β, PMA, sodium butyrate, Trichostatin A, phosphatase inhibitor cocktail, protease inhibitor cocktail and β-actin (A-1978) were purchased from Sigma-Aldrich. Rabbit polyclonal anti-phospho-P38 (sc-17852-R) or mouse monoclonal anti-phospho ERK (sc-7383) antibodies were purchased from Santa Cruz Biotechnology; anti acetyl H3 (06-599) was from Millipore-Upstate (Milan, Italy), and P21^{CIP1} (ab7960) from Abcam.

Results

Cholbut SLN inhibits CRC adhesion to HUVEC

Initially, we evaluated the internalization of cholbut SLN in the HT29 cell line by assessing the uptake of fluorescent 6-coumarin-tagged cholbut SLN. HT29 cells were allowed to attach for 24 h to glass coverslips in 24-well plates. They were then incubated for 15 min with 100 µM fluorescent cholbut SLN, washed and analysed by fluorescence microscopy. Figure 1 shows that high levels of fluorescence were detectable in the cytoplasm throughout the entire observation
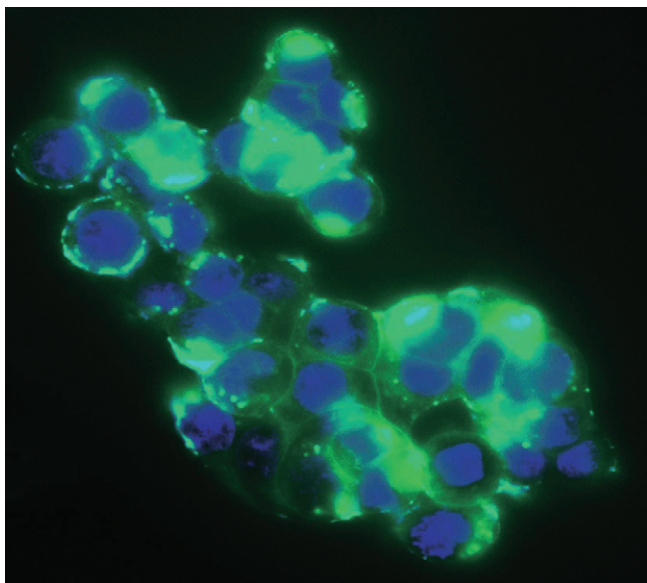
Figure 1

Microscopical analysis of HT29 cells stained with DAPI (shown in blue), as nuclear stain, after a 15 min exposure to 100 µM of fluorescent cholbut SLN (63× magnification).

period (15–60 min), which confirmed the results previously obtained on HUVEC and PMNs by confocal microscopy (Dianzani *et al.*, 2006).

We analysed the effect of cholbut SLN on adhesion of HT29 to HUVEC and compared it with the effect of the free drug, as sodium butyrate. Cholesteryl palmitate (cholpalm) SLN were used as control of the cholesteryl matrices because of their known ineffectiveness in several cell lines (Brioschi *et al.*, 2008). The cholbut concentrations used had previously been found not to be toxic for HUVEC (Dianzani *et al.*, 2006).

First, we investigated the effect of cholbut SLN on HUVEC. HUVEC were treated or otherwise with titrated amounts (0.1–100 µM) of each reagent for 24 h, washed and used in the adhesion assay with HT29 cells. Figure 2A shows that cholbut SLN inhibited HT29 adhesion to HUVEC in a concentration-dependent manner; the effect was already significant at 1 µM (about 50% inhibition), with maximal inhibition (75 ± 5%) obtained at the highest concentration (100 µM) (IC_{50} = 3.86 ± 1.03 µM). By contrast, sodium butyrate significantly inhibited adhesion only at 100 µM, whereas no significant inhibition was detected with any concentration of cholpam SLN, which showed the lack of effect exerted by both the cholesteryl matrices and the palmitate. Duration of the inhibitory effect was investigated by performing the HT29 adhesion assay on HUVEC treated for different times (2–48 h) with titrated amounts (0.1–100 µM) of cholbut SLN. The results showed that adhesion inhibition was detectable after 8 h of treatment, but only at the highest concentration of cholbut SLN, and it was maximal at 24–48 h (Figure 2B). No effect was detected after 2–4 h of treatment (data not shown). As EC adhesiveness is potentiated by pro-inflammatory cytokines, we repeated the adhesion assay using HUVEC pre-activated with 0.01 µM IL-1β for 1 h to assess the effect of cholbut SLN in an inflammatory environ-

ment. Pre-activated HUVEC were treated or otherwise with cholbut SLN for a further 24 h and used in the adhesion assay with HT29 cells. The results showed that treatment with IL-1β increased HT29 adhesion by 152 ± 6%, and cholbut SLN inhibited this adhesion in a concentration-dependent manner reaching 100% inhibition at the highest concentration (Figure 2C).

Second, we investigated the direct effect of cholbut SLN on HT29 and HCT116 cells. HT29 and HCT116 cells were treated with cholbut SLN (0.1–100 µM) for 8–48 h, washed and used on the adhesion assay on untreated HUVEC. The results showed that treatment with cholbut SLN inhibited cancer cell adhesion to a similar extent and with kinetics similar to those displayed on HUVEC. The inhibition was apparently more effective on HCT116 (Figure 3B) than on HT29 cells (Figure 3A). As these data indicated that the drug exerted its effect on both HUVEC and cancer cells, we also evaluated the overall effect of cholbut SLN acting on both cell targets. HT29 cells and HUVEC were separately treated with cholbut SLN (0.1–10 µM) for 24 h, washed and then used together in the adhesion assay. The results showed that cholbut SLN inhibited adhesion with maximal efficacy (about 70% of inhibition) at a low concentration, 0.1 µM (Figure 3C), which indicated that the effect was maximal when the drug acted on both partners of the adhesion assay.

To assess these inhibitory effects over a wider range of cancer cells, we evaluated adhesiveness of HUVEC treated with different concentrations of cholbut SLN for 24 h to other tumour cell lines, HCT116 and CaCo-2 cells (weakly and highly differentiated CRC, respectively), MFC-7 cells (breast), PC-3 cells (prostate), LM and M14 cells (melanoma). The results showed that cholbut SLN inhibited adhesion of all cell lines to an extent similar to that of HT29 (Figure 3D).

We have recently shown that a similar inhibition of tumour cell adhesion to HUVEC was also induced by the triggering of B7h, a surface receptor expressed by both HUVEC and several tumour cell lines including HT29 cells, using the T-cell receptor fusion protein, ICOS-Fc (Dianzani *et al.*, 2010). In this case, too, inhibition was exerted on both partners of the adhesion assay. To assess whether the two drugs might cooperate in inhibiting HT29 cell adhesion, HUVEC were treated for 24 h with ICOS-Fc (0.5–0.1 µM) or cholbut SLN (0.3–1 µM) or both and then used in the adhesion assay with HT29 cells. The results showed that the combination of treatments had a higher inhibitory effect than that of each single treatment, with an additive effect (Figure 4).

Cholbut SLN inhibit cell migration

A crucial component of tumour cell invasion is cell migration. To assess the effect of cholbut SLN on directional migration of tumour cells, we performed the scratch assay, an *in vitro* 'wound-healing' assay, on PC-3 cells chosen because they displayed high migratory activity in this assay. A linear scratch was performed on a confluent monolayer of PC-3 cells, which were then cultured in FCS-free medium to minimize cell proliferation with or without cholbut SLN and sodium butyrate (1–100 µM). Microscopic analysis evaluating cell capacity to migrate and fill the empty areas at different times showed that, in the absence of any drug, substantial counts of cells migrating in the wound area were detectable
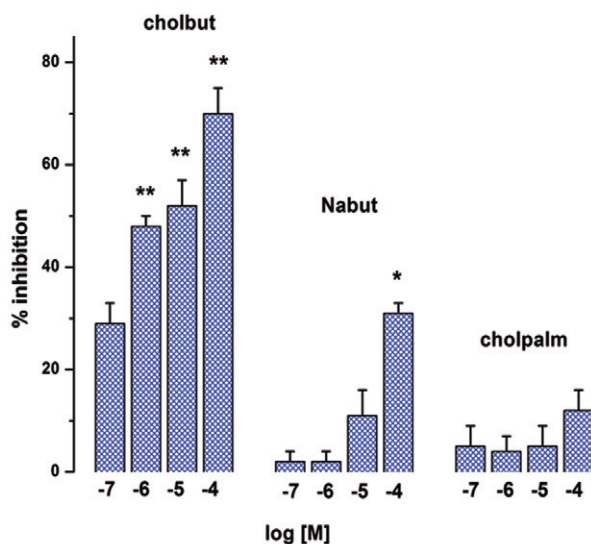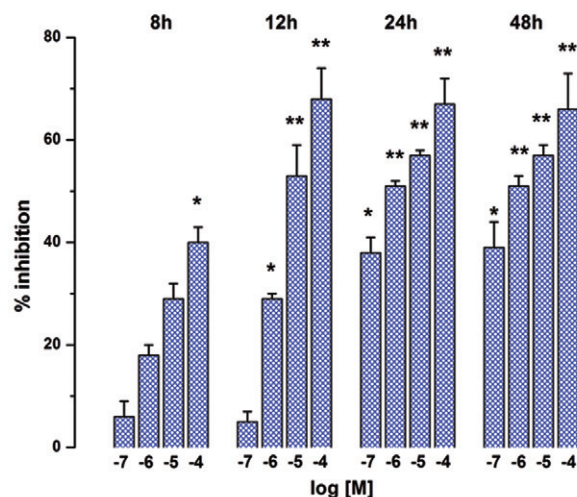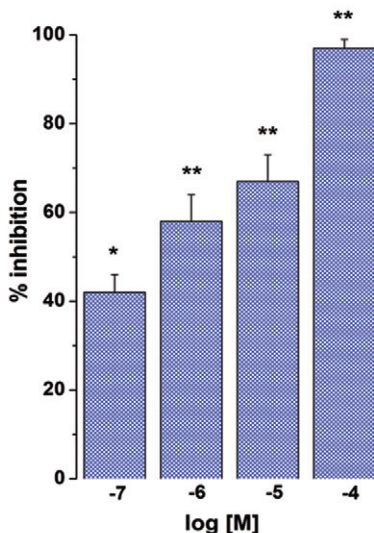
Figure 2
Effect of cholbut SLN on HUVEC adhesiveness to HT29 cells. (A) Effect of HUVEC treatment with cholbut SLN, sodium butyrate (Nabut) and cholpalm SLN on their adhesiveness to HT29 cells. HUVEC were pre-treated or otherwise with increasing concentrations of these drugs (0.1–100 μM) for 24 h and then incubated with HT29 for 1 h. Data are expressed as mean ± SEM ($n = 5$) of the percentage of inhibition versus control adhesion detected on untreated HUVEC; control adhesion was 40 ± 4 cells/microscope fields (*$P < 0.05$; **$P < 0.01$ significantly different from the control). (B) Effect of HUVEC treatment for different times with cholbut SLN on their adhesiveness to HT29 cells. HUVEC were pre-treated or otherwise with increasing concentrations of cholbut SLN (0.1–100 μM) for 8, 12, 24 or 48 h, and then incubated with HT29 cells for 1 h. Data are expressed as mean ± SEM ($n = 5$) of the percentage of inhibition versus the control adhesion (*$P < 0.05$; **$P < 0.01$ significantly different from the control). (C) Effect of treatment of IL-1β-stimulated HUVEC with cholbut SLN on their adhesiveness to HT29 cells. HUVEC were pre-treated for 1 h with 0.01 μM IL-1β, then incubated or otherwise with increasing concentrations of cholbut SLN (0.1–100 μM) for 24 h and then incubated with HT29 for 1 h. IL-1β increased HT29 adhesion by 152 ± 6%. Data are expressed as mean ± SEM ($n = 5$) of the percentage of inhibition versus control adhesion detected on stimulated HUVEC (*$P < 0.05$; **$P < 0.01$ significantly different from the control).

after 24–48 h, and treatment with cholbut SLN inhibited this migration in a concentration-dependent manner, starting at 10 μM. By contrast, no significant inhibition of migration was detected using sodium butyrate at any concentration (Figure 5A).

The effect on cell migration was further investigated using the Boyden chamber invasion assay using PC-3, HT29 and HCT116 cells, as they efficiently migrate in this assay. These cells were suspended in a FCS-free medium, seeded in the upper chamber in the presence and absence of titrated amounts of cholbut SLN or sodium butyrate (1–100 μM) and allowed to migrate for 8 h towards the lower chamber containing medium+20% FCS used as a migratory stimulus. Figure 5B shows that PC-3, HT29 and HCT116 cell migration was inhibited by about 50% and 35% upon treatment with 100 and 10 μM cholbut SLN respectively. By contrast, sodium butyrate was ineffective at any concentration.

Cholbut SLN modulate MAPK signalling and expression of E-cadherin and claudin-1

To investigate the mechanism of cholbut SLN-mediated inhibition of cell adhesiveness, we compared the expression of adhesion molecules in HT29 cells and HUVEC treated with (10–100 μM) cholbut SLN for 24 h. The surface expression of crucial adhesion molecules such as ICAM-1, ICAM-2, VCAM-1, MadCAM, CD31, E-selectin (CD62E), CD62P, CD15s (Sialyl Lewis X), Sialyl Lewis A and B7h was assessed by immunofluorescence and flow cytometry. The results showed that cholbut SLN treatment had no effect on these expression patterns, either on HUVEC or on HT29 (Table 1).

An alternative possibility was that cholbut SLN modulated the intrinsic adhesiveness of adhesion molecules without affecting their expression level. This effect might be mediated by modulation of signalling pathways involved in the spatial organization of the adhesion receptors and the cytoskeleton.
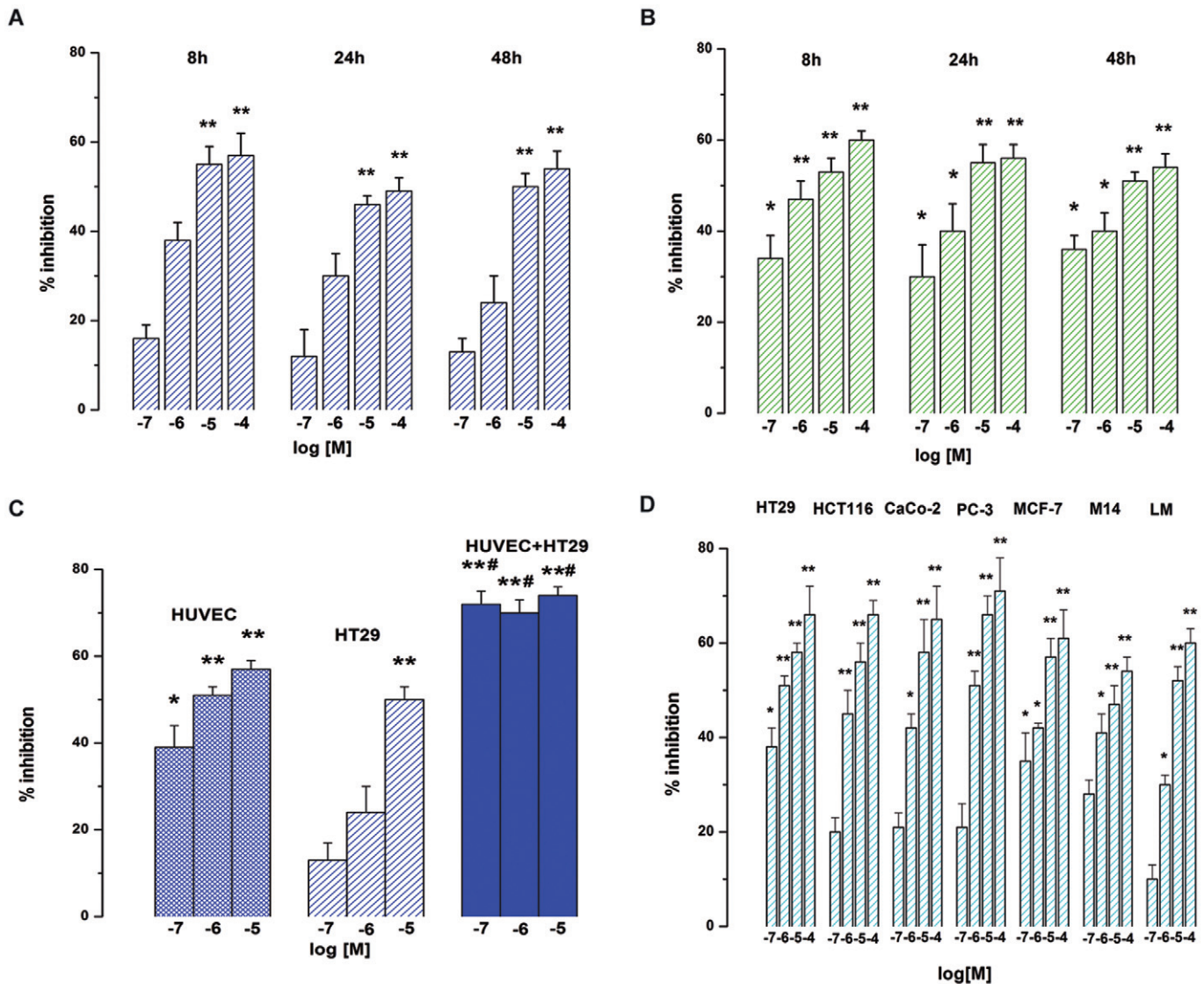
Figure 3

Effect of cholbut SLN on adhesiveness of several cell lines. (A) Effect of cholbut SLN on HT29 adhesiveness. HT29 cells were pre-treated or otherwise with increasing concentrations of cholbut SLN (0.1–100 μM) for 8, 24 or 48 h, washed, and then incubated with HUVEC for 1 h. Data are expressed as mean $\pm$ SEM ($n = 5$) of the percentage of inhibition versus the control adhesion (**$P < 0.01$ vs. the control). (B) Effect of cholbut SLN on HCT116 adhesiveness. HCT116 cells were pre-treated or otherwise with increasing concentrations of cholbut SLN (0.1–100 μM) for 8, 24 or 48 h, washed, and then incubated with HUVEC for 1 h. Data are expressed as mean $\pm$ SEM ($n = 5$) of the percentage of inhibition versus the control adhesion (*$P < 0.05$; **$P < 0.01$, significantly different from the control). (C) Additive effect of cholbut SLN on HT29 and HUVEC adhesiveness. HUVEC and HT29 were separately pre-treated or otherwise with increasing concentrations of drugs (0.1–10 μM) for 24 h, washed twice and then incubated together for 1 h. Data are expressed as mean $\pm$ SEM ($n = 5$) of the percentage of inhibition versus control adhesion detected on untreated HUVEC (*$P < 0.05$; **$P < 0.01$, significantly different from the control; #$P < 0.05$, significantly different from single treatment). (D) Effect of cholbut SLN on HUVEC adhesiveness to several tumour cell lines. HUVEC were pre-treated or otherwise with increasing concentrations of drugs (0.1–100 μM) for 24 h and then incubated with HT29, HCT116, CaCo-2, PC-3, MCF-7, M14 and LM for 1 h. Data are expressed as mean $\pm$ SEM ($n = 5$) of the percentage of inhibition versus control adhesion detected on untreated HUVEC (*$P < 0.05$; **$P < 0.01$, significantly different from the control).

The MAPK signalling pathway has been shown to play a key role in regulating tumour cell invasion (Hwang *et al.*, 2011). In line with this notion, the interaction of HT29 cells with HUVEC induces p38 and ERK phosphorylation (Tremblay *et al.*, 2006); moreover, B7h triggering inhibits this pathway and, in turn, the reciprocal adhesion of these cells. To investigate whether Cholbut SLN, too, may influence this

pathway, HUVEC, HT29 and HCT116 cells were incubated with 100 μM cholbut SLN for 8–48 h and then treated with 0.01 μM VEGF-A (HUVEC) or 0.01 μM PMA (HT29 or HCT116 cells) for 10 min to trigger the MAPK pathway (Qian *et al.*, 2006). Western blot analysis of ERK1/2 and p38 phosphorylation showed that ERK phosphorylation was induced by VEGF-A in HUVEC (Figure 6A), by PMA in HT29 (Figure 6B)
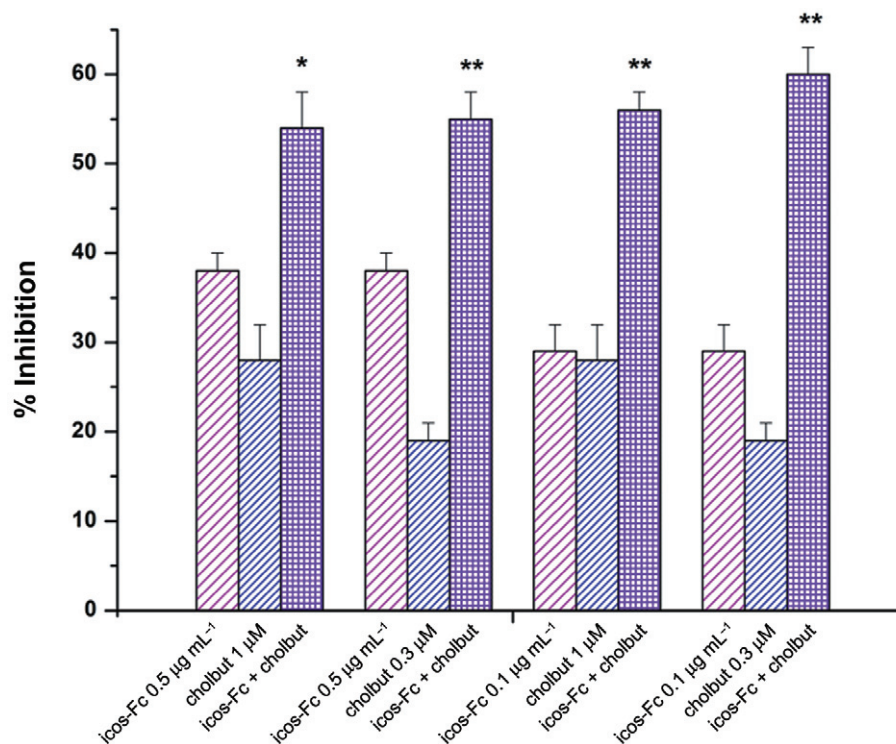
Figure 4

Additive effect of ICOS-Fc and cholbut SLN on HUVEC adhesiveness to HT29. HUVEC were pre-treated or otherwise with cholbut SLN (0.3–1 μM) and/or ICOS-Fc 0.5–0.1 μg·mL⁻¹ for 24 h, washed and then incubated with HT29 for 1 h. Data are expressed as mean ± SEM ($n = 5$) of the percentage of inhibition versus the control adhesion (cells not treated either with cholbut SLN or ICOS-Fc) (*$P < 0.05$; **$P < 0.01$, significantly different from single treatment).

Table 1

Lack of effect of cholbut SLN on expression of adhesion molecules in HT29 cells and HUVEC

Adhesion molecule	HT29 Untreated	Treated	HUVEC Untreated	Treated
ICAM-1	1.59	1.58	2.72	2.33
CD62P	1	1.08	1.21	1.22
B7h	1.5	1.48	1.57	1.26
Sialyl X	1	1.11	1.88	2.1
MadCAM	1	1.17	1.37	1.26
CD31	1.35	1.62	50	46.63
Sialyl A	1.84	1.76	2	1.22
VCAM-1	1.24	1.24	1.73	1.58
ICAM-2	1	1.15	4.57	3.85
CD62E	–	–	2.89	2.91

HT29 and HUVEC cells were treated with 100 μM of cholbut SLN for 24 h and stained for the adhesion molecules listed. The results are shown as the fluorescence signal from cells (as mean flourescence intensity), with and without treatment with cholbut SLN ($n = 3$).

and in HCT116 cells (Figure 6C), and that it was time-dependently inhibited by treatment with cholbut SLN. Similarly, p38 phosphorylation was induced by VEGF-A in HUVEC, and it was inhibited by treatment with cholbut SLN for 24 h or 48 h (Figure 6D). By contrast, PMA did not induce p38 phosphorylation in HT29 or HCT116 cells, and this was not changed by treatment with cholbut SLN (data not shown).

To further assess involvement of the MAPK pathway in the cholbut SLN-mediated inhibition of tumour cell adhesion to HUVEC, we performed the adhesion assay, using HUVEC treated for 24 h with and without SB203580 (10 μM) or PD98059 (10 μM), p38 and ERK inhibitors, respectively, in the presence and absence of cholbut SLN (10 μM). Results showed that PD98059 and SB203580 inhibited HT29 adhesion by 33 ± 5% and 38 ± 4%, respectively, and this inhibition was not increased by treatment of the cells with cholbut SLN. The same results were obtained using this approach in the migration assay (37 ± 8% and 40 ± 7% respectively).

Cadherins and claudin-1 (CLDN1) are also involved in cell migration and invasiveness by modulating the organization of the cytoskeleton and tight junctions (Gumbiner, 1996). In CRC, a low expression of E-cadherin is correlated with poor outcome and increased invasiveness (Christofori and Semb, 1999), and claudin-1 is highly expressed, especially at the metastatic lesion level (Dhawan *et al.*, 2005).
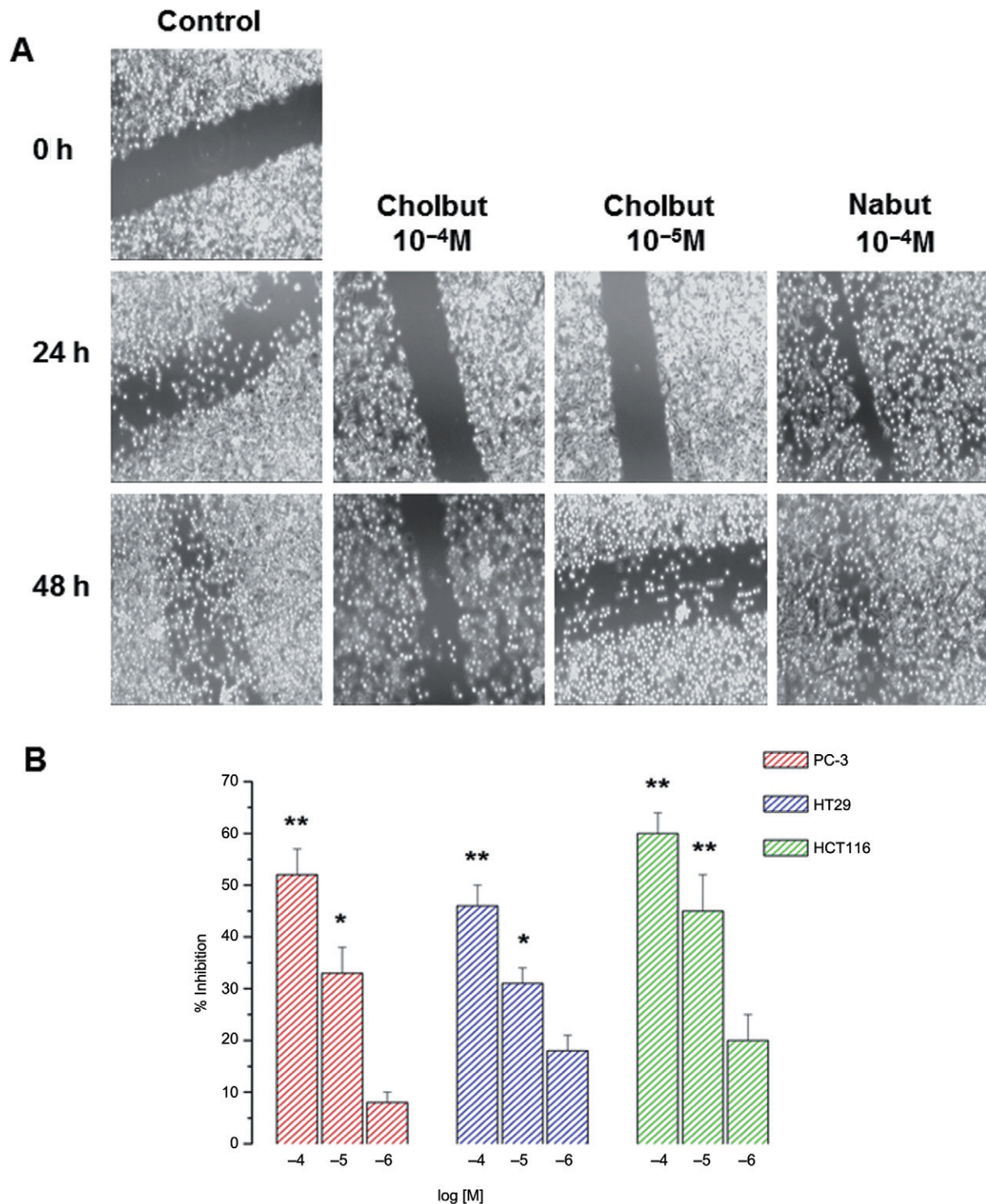
Figure 5

Inhibition of tumour cell motility and invasion by cholbut SLN. (A) Inhibition of PC-3 cell motility evaluated by a scratch 'wound-healing' assay. PC-3 cells were grown to confluence on 6 well-plates. A scratch was made through the cell layer using a pipette tip; the cells were washed and then treated with cholbut SLN (10-100 μM) or sodium butyrate (Nabut; 100 μM) for 24–48 h. Microphotographs of the wounded area were taken immediately after the scratch was made (0 h) and 24–48 h later, in order to monitor cell migration into the wounded area ($n = 3$). (B) Inhibition of tumour cell invasion by a Boyden chamber assay. PC-3, HT29 and HCT116 cells were plated onto the apical side of Matrigel-coated filters in 50 μL of cholbut SLN of (1–100 μM) for 8 h. The cells migrated to the bottom of the filters were stained using crystal violet and counted (five fields of each triplicate filters) using an inverted microscope. Control migration was 34 ± 4 cells/microscope fields. Data are expressed as mean $\pm$ SEM ($n = 5$) of the percentage of inhibition versus the control migration (*$P < 0.05$; **$P < 0.01$ significantly different from the control).
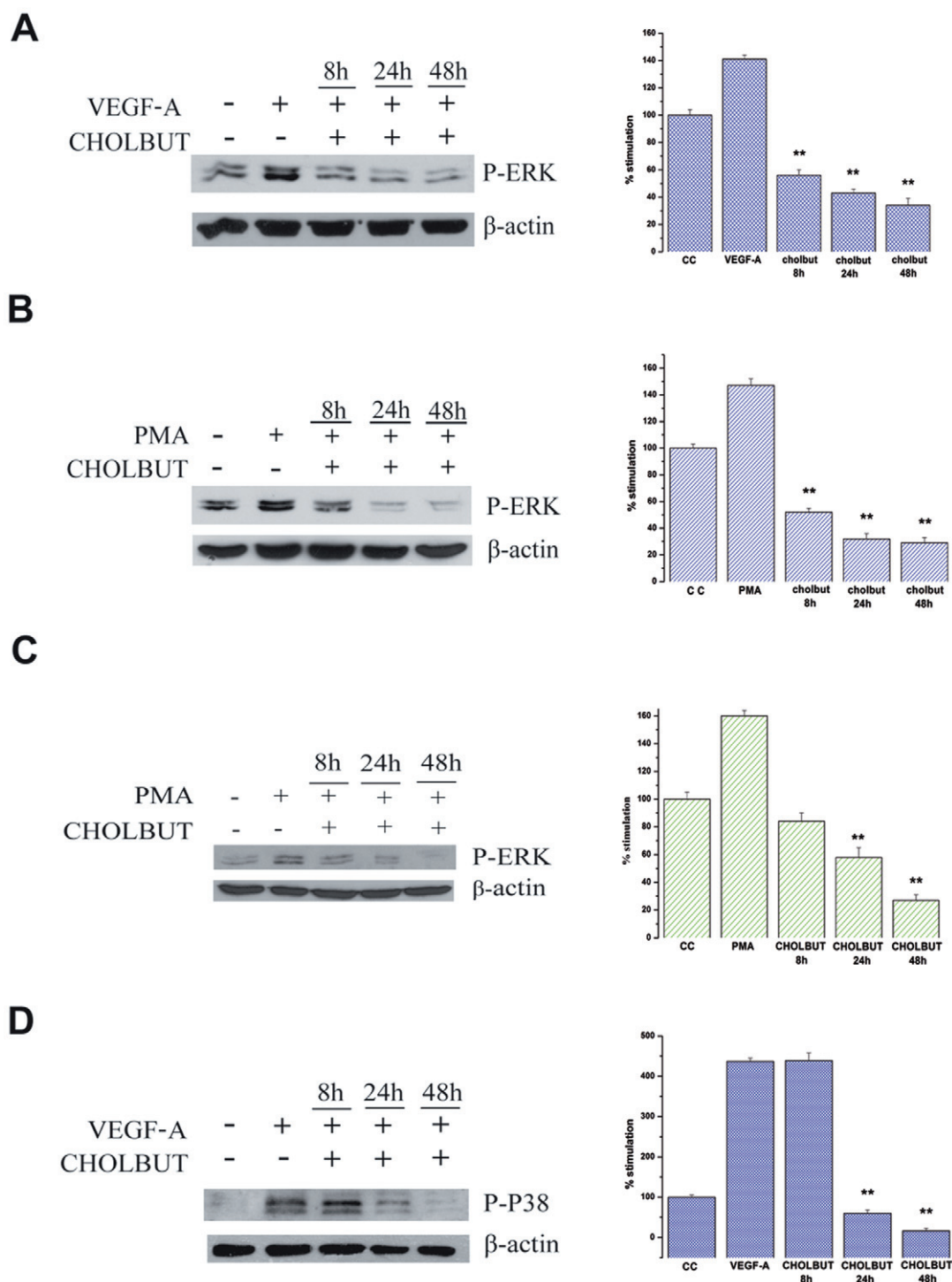
Figure 6

Effect of cholbut SLN on ERK and p38 phosphorylation induced in HUVEC, HT29 and HCT116 cells by activation stimuli. (A, D) HUVEC were treated with 100 μM cholbut SLN for 8, 24 or 48 h and subsequently incubated with fresh media containing (0.01 μM) VEGF-A in order to stimulate ERK (A) and p38 (D) phosphorylation (as p-ERK, p-p38), which was then evaluated by Western blot in the cell lysates; the same blots were also probed with anti β-actin antibody as a control. Left: Western blot analysis from a representative experiment. Right: Densitometric analysis of ERK and p38 phosphorylation expressed in arbitrary units from three independent experiments. (B, C) Effect on HT29 (B) and HCT116 (C) cells. HT29 or HCT116 cells were treated with 100 μM cholbut SLN for 8, 24 or 48 h and subsequently incubated with fresh media containing (0.01 μM) PMA in order to stimulate ERK phosphorylation, which was then evaluated by Western blot in the cell lysates; the same blots were also probed with anti β-actin antibody as a control. Left: Western blot analysis from a representative experiment. Right: Densitometric analysis of ERK phosphorylation expressed in arbitrary units of three independent experiments. Data are expressed as mean $\pm$ SEM ($n = 3$) of the percentage of inhibition versus the control (**$P < 0.01$, significantly different from the control).
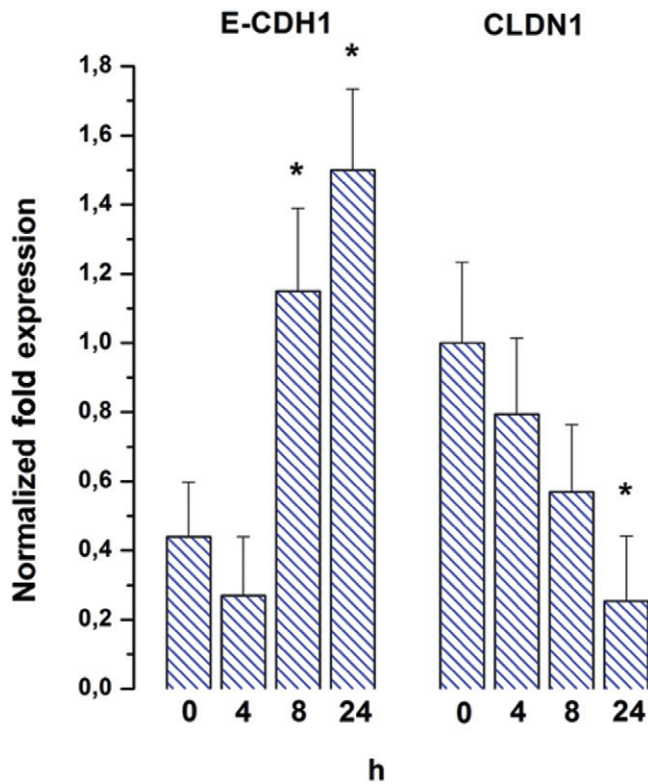
Figure 7

Time-dependent expression of the E-cadherin and claudin-1 mRNA after treatment with cholbut SLN. E-cadherin (*CDH1*) and claudin-1 (*CLDN1*) mRNA expression in HT29 cells were analysed by real-time PCR at 4, 8 and 24 h after incubation with 100 μM cholbut SLN. The housekeeping *GAPDH* gene transcript was used as reference to normalize mRNA levels. Data are expressed as mean ± SD ($n = 3$) (*$P < 0.05$, significantly different from the control).

Moreover, sodium butyrate has been shown to increase expression of E-cadherin and decrease expression of claudin-1 in CRC cell lines (Barshishat *et al*., 2000; Schmalhofer *et al*., 2009). To assess the effect of cholbut SLN on expression of E-cadherin and claudin-1, HT29 and HUVEC cells were treated with 100 μM cholbut SLN, and expression of the E-cadherin mRNA was assessed by real-time PCR at different times. A significant increase of E-cadherin mRNA was detected in HT29 cells after 8–24 h of treatment with cholbut SLN, whereas a significant decrease of claudin-1 mRNA was detected after 24 h (Figure 7). By contrast, no effect was detected in HUVEC (data not shown).

Cholbut SLN does not induce H3-hyperacetylation and P21^CIP1

The anti-tumour effects of sodium butyrate may depend on its HDAC inhibitor activity. To determine whether cholbut SLN maintained this activity in HT29 cells, we compared the capacities of sodium butyrate, cholbut SLN and Trichostatin A (a known HDAC inhibitor) to induce hyperacetylation of the H3 histone and expression of the cell cycle inhibitor P21^CIP1, which are features of HDAC inhibitor activity (Druesne *et al*., 2004). The results showed that treatment of
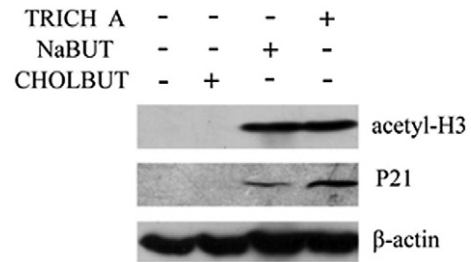

Figure 8

Effect of cholbut SLN, sodium butyrate (Nabut) and Trichostatin A (Trich A) on acetyl-H3 and p21^CIP1 expression level. HT29 cells were treated with 5 mM sodium butyrate, or 0.1 μM Trichostatin A, or 100 μM cholbut SLN, and the expression levels of acetyl-H3 and p21^CIP1 were analysed by Western blot in the cell lysates; the same blots were also probed with anti-β-actin antibody as a control ($n = 3$).

HT29 cells with either 5 mM sodium butyrate or 0.1 μM Trichostatin A-induced hyperacetylation of H3 and expression of P21^CIP1, whereas 100 μM cholbut SLN had no effect (Figure 8); 1 mM cholbut SLN also had no effect (data not shown). These results suggest that cholbut SLN had no HDAC inhibitor activity at these concentrations. Similar results have been obtained using PC-3 cells.

Discussion and conclusion

This work has shown that cholbut SLN inhibited the adhesion of several tumour cell lines to EC by acting on both EC and tumour cells, and that it inhibited tumour cell migration. These effects were not attributable to drug toxicity as the proliferation of both EC and tumour cells was not affected in the concentration range affecting cell adhesion.

Key players in tumour cell adhesion to EC are selectins with their mucin-like ligands, and integrins, whose ligands mostly belong to the immunoglobulin superfamily. But several other adhesion molecules may also be involved. Cell adhesiveness may be modulated not only by the expression levels of the adhesion molecules but also by their spatial distribution in specialized membrane structures, which may compartmentalize different adhesion molecules to specific regions of the plasma membrane and favour their cooperation with other receptors and signalling molecules. This topographic organization requires a finely regulated cellular cytoskeleton that also enables the recruitment of signalling intermediates and second messengers that lead to cell activation (Barreiro *et al*., 2005; 2007).

Our data showed that the adhesion inhibition mediated by cholbut SLN was relatively delayed and long-lasting, since it was detectable 8 h after treatment with the drug and lasted up to 48 h. This was not due to a slow uptake of the drug because substantial uptake into the cells was already detectable after 15 min. Brioschi *et al*., 2008 have reported that cholbut SLN are rapidly internalized by phagocytosis in glioma cells, where they persist for several days and possibly undergo a complex intracellular metabolism, as suggested by their different subcellular localizations in the subsequent days.

One possibility was that the cholbut SLN anti-adhesive effects in our experiments were mediated by modulation of expression of adhesion receptors, but this seemed not to be the case because flow cytometry did not detect expression of adhesion receptors in EC and tumour cells. By contrast, we found that cholbut SLN induced up-modulation of E-cadherin and down-modulation of claudin-1 at the mRNA level, which is in line with data previously reported for sodium butyrate (Barshishat et al., 2000), and may be relevant to the anti-adhesive effects because these proteins are involved in organization of the cytoskeleton and influence cell adhesiveness and motility. Indeed, low expression of E-cadherin has been correlated with poor outcome and high invasiveness in CRC in vivo (Christofori and Semb, 1999), and enforced expression of E-cadherin has been shown to inhibit cell invasiveness in vitro (Behrens, 1999). Furthermore, claudin-1 expression has been positively correlated with CRC progression, invasion and metastasis dissemination (Dhawan et al., 2005).

Cholbut SLN also inhibited phosphorylation of ERK and p38, without affecting their expression. This effect, too, was intriguing, since ERK and p38 have been involved in several signalling pathways modulating tumour cell adhesion and migration, possibly by influencing membrane distribution, and the clustering of several adhesion receptors and their connection with the cytoskeleton (Kiely et al., 2003; Van Slambrouck et al., 2009). Moreover, ERK signalling influences the organizational status of α_2 integrin and has been correlated with tumour invasiveness (Buda et al., 2003; Sawhney et al., 2006). In line with a role of the MAPK pathway in the cholbut SLN effect, we found that MAPK inhibitors decreased tumour cell adhesion and migration, and that this effect was not potentiated by cholbut SLN. By contrast, cholbut displayed an additive effect on the adhesion inhibition induced by ICOS-Fc-mediated triggering of B7h, which also inhibited MAPK phosphorylation. However, the effect of B7h triggering was already detectable after a few minutes, which suggested that it used mechanisms partly different from cholbut SLN, whose effect was delayed for several hours. This finding is intriguing because it suggests that simultaneous use of cholbut SLN and ICOS-Fc may substantially improve the effectiveness of these drugs, given that relatively low doses of cholbut SLN (0.03 μM) induced a striking inhibition (about 60%) of cell adhesion when used in the presence of ICOS-Fc. These data match those showing that, in several CRC cell lines and primary tumours, constitutively activated MAPK have been associated with enhanced cell proliferation and minor survival (Kuno et al., 1998; Hoshino et al., 1999; Xu et al., 2009), and these kinases have been regarded as an attractive target for anticancer therapies (Sebolt-Leopold and Herrera, 2004; Kohno and Pouyssegur, 2006). Moreover, alterations in cell signalling pathways, including that of MAPK, may play a role in the complex mechanisms underlying tumour resistance to chemotherapeutic agents (Boldt et al., 2002), and inhibition of the MAPK pathway has been shown to result in the down-regulation of the P-glycoprotein involved in multidrug resistance, with a consequent decrease of multidrug resistance itself (Katayama et al., 2007).

The integration of Rho family GTPase and ERK signalling is also important for tumour cell motility (Pullikuth and Catling, 2010; Adachi et al., 2011). But the Rho family seemed to be not involved in the cholbut SLN effect on migration because experiments showed that the Rho kinase inhibitor Y-27632, stimulating cancer cell migration, did not influence the capacity of cholbut SLN to inhibit tumour cell migration (data not shown).

A key finding is that cholbut SLN inhibited adhesion at concentrations that were 1000 times lower than those active for free butyrate (0.1–1 μM vs. 0.1–1 mM), which suggested that cholbut SLN were an effective delivery system for the drug. In the colon lumen, butyrate is present at high concentrations (about 2–3 mM), which would reach pharmacological effectiveness, but colon cancer cells must develop mechanisms to escape these effects, since they grow despite these concentrations. Several studies have indicated that expression of the anion transporters, monocarboxylate transporter 1 (MCT1) and sodium-coupled monocarboxylate transporter 1 (SMCT1) (Davis et al., 2008), involved in specific carrier-mediated transport of SCFA anions, are significantly down-regulated in colon cancer cells, which would decrease the intracellular concentration of butyrate and deregulate butyrate-induced gene expression. In addition, expression of SMCT1 is often decreased also in stomach, thyroid, prostate, breast and brain cancers (Gupta et al., 2006). We suggest that cholbut SLN may overcome these transport defects by entering into the cells without a specific carrier-mediated transport, and the cholbut SLN entered may prevent rapid elimination from the cell by locating far away from the transmembrane efflux pumps responsible for drug elimination (Hamer et al., 2008).

A second finding is that cholbut SLN effects may be partly different from those displayed by sodium butyrate, since both drugs inhibited adhesion but only the former also inhibited migration, whereas only the latter displayed HDAC inhibitor activity. In line with a partly different effect of the two drugs, cholbut SLN had been shown to exert anti-proliferative and pro-apoptotic effects at lower doses and shorter treatment times than sodium butyrate in several tumour cell lines (Brioschi et al., 2008). Moreover, cholbut SLN caused a cell cycle arrest in the G_1 phase in myeloid cell lines, mainly ascribed to c-myc repression and/or $p21^{WAF1}$ up-regulation, but it caused an unexplained arrest in the G_2 phase in lymphoid cell lines (Serpe et al., 2004).

Current anticancer treatments mostly target tumour cell proliferation and are relatively ineffective on slowly proliferating tumour cells, which may survive and give rise to new tumours even after several years (Entschladen et al., 2004). Moreover, tumour cell adhesiveness and migration play a crucial role in metastatic dissemination of cancer (Hayot et al., 2006), and migrating cells often display a decreased proliferation rate and are thus relatively insensitive to standard chemotherapies (Giese et al., 2003; Haga et al., 2003; Douma et al., 2004). Therefore, a focus of innovative cancer therapies is to inhibit the spreading of tumour cells by targeting their migratory activity mainly through use of antagonists against the adhesion molecules involved in adhesion to the extra-cellular matrix (Sawyer, 2004) or against the proteases facilitating migration by degrading the extra-cellular matrix (Zucker et al., 2000; Coussens et al., 2002; Overall and López-Otín, 2002). Unfortunately, no tested compounds have to date reached the market because of poor in vivo

anti-tumour activity, unsuitable therapeutic index or rapid development of chemoresistance.

The application of nanotechnology to drug delivery has already had a significant impact on many areas of medicine. Currently, more than 20 nanoparticle therapeutic agents are in clinical use, and they validate the ability of nanoparticles to improve the therapeutic index of drugs. In addition to the nanoparticles already approved, several other nanoparticle platforms are currently in preclinical and clinical development, including liposomes, polymeric micelles, dendrimers, quantum dots, gold nanoparticles and ceramic nanoparticles (Zhang *et al.*, 2008).

In conclusion, our data indicated that cholbut SLN may be an effective anti-metastatic agent acting on both EC and tumour cells, and that it may remedy some of the pharmacological weaknesses of other compounds. Moreover, preliminary experiments did not detect any *in vivo* toxicity of cholbut SLN in mice upon delivery either p.o. or i.v. (oral LD_{50} ≥1000 mg·kg^{-1}; i.v. LD_{50} ≥400 mg·kg^{-1}), but further *in vivo* study is required to assess the effect of repeated administration. Therefore, a drug like cholbut SLN, which affects cancer cells, acting on several fronts and without severe toxic effects, may be a valuble tool in cancer therapy because it acts on several aspects of tumour progression with minimal toxicity on normal cells.

Acknowledgements

Conflict of interest

P Gasco and N Vivenza are employees of Nanovector s.r.l.

References

Adachi S, Yasuda I, Nakashima M, Yamauchi T, Yoshioka T, Okano Y *et al.* (2011). Rho-kinase inhibitor upregulates migration by altering focal adhesion formation via the Akt pathway in colon cancer cells. Eur J Pharmacol 650: 145–150.

Barreiro O, Yáñez-Mó M, Sala-Valdés M, Gutiérrez-López MD, Ovalle S, Higginbottom A *et al.* (2005). Endothelial tetraspanin microdomains regulate leukocyte firm adhesion during extravasation. Blood 105: 2852–2861.

Barreiro O, De la Fuente H, Mittelbrunn M, Sánchez-Madrid F (2007). Functional insights on the polarized redistribution of leukocyte integrins and their ligands during leukocyte migration and immune interactions. Immunol Rev 218: 147–164.

Barshishat M, Polak-Charcon S, Schwartz B (2000). Butyrate regulates E-cadherin transcription, isoform expression and intracellular position in colon cancer cells. Br J Cancer 82: 195–203.

Behrens J (1999). Cadherins and catenins: role in signal transduction and tumor progression. Cancer Metastasis Rev 18: 15–30.

Boldt S, Weidle UH, Kolch W (2002). The role of MAPK pathways in the action of chemotherapeutic drugs. Carcinogenesis 23: 1831–1838.

Brioschi A, Zara GP, Calderoni S, Gasco MR, Mauro A (2008). Cholesterylbutyrate solid lipid nanoparticles as a butyric acid prodrug. Molecules 13: 230–254.

Buda A, Qualtrough D, Jepson MA, Martines D, Paraskeva C, Pignatelli M (2003). Butyrate downregulates alpha2beta1 integrin: a possible role in the induction of apoptosis in colorectal cancer cell lines. Gut 52: 729–734.

Bustin SA, Benes V, Garson JA, Hellemans J, Huggett J, Kubista M *et al.* (2009). The MIQE guidelines: minimum information for publication of quantitative real-time PCR experiments. Clin Chem 55: 611–622.

Christofori G, Semb H (1999). The role of the cell-adhesion molecule E-cadherin as a tumour-suppressor gene. Trends Biochem Sci 24: 73–76.

Coussens LM, Fingleton B, Matrisian LM (2002). Matrix metalloproteinase inhibitors and cancer: trials and tribulations. Science 295: 2387–2392.

Cummings JH (1981). Short chain fatty acids in the human colon. Gut 22: 763–779.

Davis ME, Chen ZG, Shin DM (2008). Nanoparticle therapeutics: an emerging treatment modality for cancer. Nat Rev Drug Discov 7: 771–782.

Delzenne N, Cherbut C, Neyrinck A (2003). Prebiotics: actual and potential effect in inflammatory and malignant colonic disease. Curr Opin Clin Nutr Metab Care 6: 581–586.

Dhawan P, Singh AB, Deane NG, No Y, Shiou SR, Schmidt C *et al.* (2005). Claudin-1 regulates cellular transformation and metastatic behavior in colon cancer. J Clin Invest 115: 1765–1776.

Dianzani C, Cavalli R, Zara GP, Gallicchio M, Lombardi G, Gasco MR *et al.* (2006). Cholesteryl butyrate solid lipid nanoparticles inhibit adhesion of human neutrophils to endothelial cells. Br J Pharmacol 148: 648–656.

Dianzani C, Minelli R, Mesturini R, Chiocchetti A, Barrera G, Boscolo S *et al.* (2010). B7h triggering inhibits umbelical vascular endothelial cell adhesiveness to tumor cell lines and polymorphonuclear cells. J Immunol 185: 3970–3979.

Dianzani U, Malavasi F (1995). Lymphocyte adhesion to endothelium. Crit Rev Immunol 15: 167–200.

Douma S, Van Laar T, Zevenhoven J, Meuwissen R, Van Garderen E, Peeper DS (2004). Suppression of anoikis and induction of metastasis by the neurotrophic receptor TrkB. Nature 430: 1034–1039.

Druesne N, Pagniez A, Mayeur C, Thomas N, Cherbuy C, Duée PH *et al.* (2004). Diallyl disulfide (DADS) increases histone acetylation and p21 (waf1/cip1) expression in human colon tumor cell lines. Carcinogenesis 25: 1227–1236.

Entschladen F, Drell TL, Lang K, Joseph J, Zaenker KS (2004). Tumour-cell migration, invasion, and metastasis: navigation by neurotransmitters. Lancet Oncol 5: 254–258.

Gasco MR (2001). Solid lipid nanoparticles for drug delivery. Pharm Technol Eur 13: 32–41.

Gasco MR (2004). Solid lipid nanospheres suitable to a fast internalization into cells. EP 1133286, (24/11/2004) – U.S. 6.685.960 (3/02/2004).

Giese A, Bjerkvig R, Berens ME, Westphal M (2003). Cost of migration: invasion of malignant gliomas and implications for treatment. J Clin Oncol 21: 1624–1636.

Giovannucci E, Stampfer MJ, Colditz G, Rimm EB, Willett WC (1992). Relationship of diet to risk of colorectal cancer adenoma in man. J Natl Cancer Inst 84: 91–98.

Gonçalves P, Araújo JR, Pinho MJ, Martel F (2009). Modulation of butyrate transport in Caco-2 cells. Naunyn Schmiedebergs Arch Pharmacol 379: 325–336.

Gumbiner BM (1996). Cell adhesion: the molecul basis of tissue architecture and morphogenesis. Cell 84: 345–357.

Gupta N, Martin PM, Prasad PD, Ganapathy V (2006). SLC5A8 (SMCT1)-mediated transport of butyrate forms the basis for the tumor suppressive function of the transporter. Life Sci 78: 2419–2425.

Haga A, Funasaka T, Niinaka Y, Raz A, Nagase H (2003). Autocrine motility factor signaling induces tumor apoptotic resistance by regulations Apaf-1 and Caspase-9 apoptosome expression. Int J Cancer 107: 707–714.

Hamer HM, Jonkers D, Venema K, Vanhoutvin S, Troost FJ, Brummer RJ (2008). Review article: the role of butyrate on colonic function. Aliment Pharmacol Ther 15: 104–119.

Hayot C, Debeir O, Van Ham P, Van Damme M, Kiss R, Decaestecker C (2006). Characterization of the activities of actin-affecting drugs on tumor cell migration. Toxicol Appl Pharmacol 211: 30–40.

Hoshino R, Chatani Y, Yamori T, Tsuruo T, Oka H, Yoshida O *et al*. (1999). Constitutive activation of the 41-/43-kDa mitogen-activated protein kinase signaling pathway in human tumors. Oncogene 18: 813–822.

Hwang YP, Yun HJ, Kim HG, Han EH, Choi JH, Chung YC *et al*. (2011). Suppression of phorbol-12-myristate-13-acetate-induced tumor cell invasion by piperine via the inhibition of PKCα/ERK1/2-dependent matrix metalloproteinase-9 expression. Toxicol Lett 203: 9–19.

Katayama K, Yoshioka S, Tsukahara S, Mitsuhashi J, Sugimoto Y (2007). Inhibition of the mitogen-activated protein kinase pathway results in the down-regulation of P-glycoprotein. Mol Cancer Ther 6: 2092–2102.

Kiely JM, Hu Y, García-Cardeña G, Gimbrone MA (2003). Lipid raft localization of cell surface E-selectin is required for ligation-induced activation of phospholipase C gamma. J Immunol 171: 3216–3224.

Kobayashi H, Tan EM, Fleming SE (2003). Sodium butyrate inhibits cell growth and stimulates p21WAF1/CIP1 protein in human colonic adenocarcinoma cells independently of p53 status. Nutr Cancer 46: 202–211.

Kohno M, Pouyssegur J (2006). Targeting the ERK signaling pathway in cancer therapy. Ann Med 38: 200–211.

Kuno Y, Kondo K, Iwata H, Senga T, Akiyama S, Ito K *et al*. (1998). Tumor-specific activation of mitogen-activated protein kinase in human colorectal and gastric carcinoma tissues. Jpn J Cancer Res 89: 903–909.

Laferrière J, Houle F, Taher MM, Valerie K, Huot J (2001). Transendothelial migration of colon carcinoma cells requires expression of E-selectin by endothelial cells and activation of stress-activated protein kinase-2 (SAPK2/p38) in the tumor cells. J Biol Chem 276: 33762–33772.

Laferrière J, Houle F, Huot J (2004). Adhesion of HT-29 colon carcinoma cells to endothelial cells requires sequential events involving E-selectin and integrin beta4. Clin Exp Metastasis 21: 257–264.

Ley K, Laudanna C, Cybulsky MI, Nourshargh S (2007). Getting to the site of inflammation: the leukocyte adhesion cascade updated. Nat Rev Immunol 7: 678–689.

Manjunath K, Reddy JS, Venkateswarlu V (2005). Solid lipid nanoparticles as drug delivery systems. Methods Find Exp Clin Pharmacol 27: 127–144.

Matsumura Y, Kataoka K (2009). Preclinical and clinical studies of anticancer agent-incorporating polymer micelles. Cancer Sci 100: 572–579.

Minucci S, Pelicci PG (2006). Histone deacetylase inhibitors and the promise of epigenetic (and more) treatments for cancer. Nat Rev Cancer 6: 38–51.

O'Neil BH, Goldberg RM (2008). Innovations in chemotherapy for metastatic colorectal cancer: an update of recent clinical trials. Oncologist 13: 1074–1083.

Overall CM, López-Otín C (2002). Strategies for MMP inhibition in cancer: innovations for the post-trial era. Nat Rev Cancer 2: 657–672.

Pellizzaro C, Coradini D, Morel S, Ugazio E, Gasco MR, Daidone MG (1999). Cholesteryl butyrate in solid lipid nanospheres as an alternative approach for butyric acid delivery. Anticancer Res 19: 3921–3926.

Pullikuth AK, Catling AD (2010). Extracellular signal-regulated kinase promotes rho-dependent focal adhesion formation by suppressing p190A RhoGAP. Mol Cell Biol 30: 3233–3248.

Qian DZ, Kato Y, Shabbeer S, Wei Y, Verheul HMW, Salumbides B *et al*. (2006). Targeting tumor angiogenesis with histone deacetylase inhibitors: the hydroxamic acid derivative LBH589. Clin Cancer Res 12: 634–642.

Salomone B, Ponti R, Gasco MR, Ugazio E, Quaglino P, Osella-Abate S *et al*. (2001). In vitro effects of cholesteryl butyrate solid lipd nanospheres as a butyric acid prodrug on melanoma cells: evaluation of antiproliferative activity and apoptosis induction. Clin Exp Metastasis 18: 663–673.

Sawhney RS, Cookson MM, Omar Y, Hauser J, Brattain MG (2006). Integrin alpha2-mediated ERK and calpain activation play a critical role in cell adhesion and motility via focal adhesion kinase signaling: identification of a novel signaling pathway. J Biol Chem 281: 8497–8510.

Sawyer TK (2004). Cancer metastasis therapeutic targets and drug discovery: emerging small-molecule protein kinase inhibitors. Expert Opin Investig Drugs 13: 1–19.

Scharlau D, Borowicki A, Habermann N, Hofmann T, Klenow S, Miene C *et al*. (2009). Mechanisms of primary cancer prevention by butyrate and other products formed during gut flora-mediated fermentation of dietary fibre. Mutat Res 682: 39–53.

Schmalhofer O, Brabletz S, Brabletz T (2009). E-cadherin, beta-catenin, and ZEB1 in malignant progression of cancer. Cancer Metastasis Rev 28: 151–166.

Sebolt-Leopold JS, Herrera R (2004). Targeting the mitogen-activated protein kinase cascade to treat cancer. Nat Rev Cancer 4: 937–947.

Serpe L, Laurora S, Pizzimenti S, Ugazio E, Ponti R, Canaparo R *et al*. (2004). Cholesteryl butyrate solid lipid nanoparticles as a butyric acid pro-drug: effects on cell proliferation, cell cycle distribution and c-myc expression in human leukemic cells. Anticancer Drugs 15: 525–536.

Serpe L, Canaparo R, Daperno M, Sostegni R, Martinasso G, Muntoni E *et al*. (2010). Solid lipid nanoparticles as anti-inflammatory drug delivery system in a human inflammatory bowel disease whole-blood model. Eur J Pharm Sci 39: 428–436.

Tremblay PL, Auger FA, Huot J (2006). Regulation of transendothelial migration of colon cancer cells by E-selectin-mediated activation of p38 and ERK MAP kinases. Oncogene 25: 6563–6573.

Van Slambrouck S, Jenkins AR, Romero AE, Steelant WF (2009). Reorganization of the integrin alpha2 subunit controls cell adhesion and cancer cell invasion in prostate cancer. Int J Oncol 34: 1717–1726.

Weiss L (1990). Metastatic inefficiency. Adv Cancer Res 54: 159–211.

Westesen K, Bunjes H, Kock HJ (1997). Physicochemical characterization of lipid nanoparticles and evaluation of their drug loading capacity and sustained release potential. J Control Release 48: 223–236.

Wollowski I, Reckemmer G, Pool-Zobel BL (2001). Protective role of probiotics and prebiotics in colon cancer. Am J Clin Nutr 73: 451S–455S.

Xu R, Sato N, Yanai K, Akiyoshi T, Nagai S, Wada J *et al*. (2009). Enhancement of paclitaxel-induced apoptosis by inhibition of mitogen-activated protein kinase pathway in colon cancer cells. Anticancer Res 29: 261–270.

Zhang L, Gu FX, Chan JM, Wang AZ, Langer RS, Farokhzad OC (2008). *Nanoparticles* in medicine: therapeutic applications and developments. Clin Pharmacol Ther 83: 761–769.

Zucker S, Cao J, Chen WT (2000). Critical appraisal of the use of matrix metalloproteinase inhibitors in cancer treatment. Oncogene 19: 6642–6650.